Monthly Notices
of the
ROYAL ASTRONOMICAL SOCIETY

Mon. Not. R. Astron. Soc. **423,** 294–303 (2012) doi:10.1111/j.1365-2966.2012.20872.x

Star formation history and environment of the dwarf galaxy UGCA 92

Lidia Makarova,[1,2]★ Dmitry Makarov[1,2,3,4] and Sergey Savchenko[5]

[1]*Special Astrophysical Observatory, Nizhniy Arkhyz, Karachai-Cherkessia 369167, Russia*
[2]*Isaac Newton Institute of Chile, SAO Branch, Nizhniy Arkhyz, Karachai-Cherkessia 369167. Russia*
[3]*Université Lyon 1, Villeurbanne, F-69622, France*
[4]*CRAL, Observatoire de Lyon, St Genis Laval, F-69561, France*
[5]*Astronomical Institute, St Petersburg State University, Universitetskii pr. 28, 198504 St Petersburg, Stary Peterhof, Russia*

Accepted 2012 March 2. Received 2012 February 22; in original form 2011 September 4

ABSTRACT

We present a quantitative star formation history of the nearby dwarf galaxy UGCA 92. This irregular dwarf is situated in the vicinity of the Local Group of galaxies in a zone of strong Galactic extinction (IC 342 group of galaxies). The galaxy was resolved into stars, including the old red giant branch, with *HST*/ACS. We constructed a model of the resolved stellar populations and measured the star formation rate and metallicity as functions of time. The main star formation activity period occurred about 8–14 Gyr ago. These stars are mostly metal-poor, with a mean metallicity [Fe/H] ~ -1.5 to -2.0 dex. About 84 per cent of the total stellar mass was formed during this event. There are also indications of recent star formation starting about 1.5 Gyr ago and continuing to the present. The star formation in this event shows moderate enhancement from ∼200 to 300 Myr ago. It is very likely that the ongoing star formation period has a higher metallicity of about -0.6 to -0.3 dex. UGCA 92 is often considered to be the companion to the starburst galaxy NGC 1569. A comparison of our star formation history of UGCA 92 with that of NGC 1569 reveals no causal or temporal connection between recent star formation events in these two galaxies. We suggest that the starburst phenomenon in NGC 1569 is not related to the galaxy's closest dwarf neighbours and does not affect their star formation history.

Key words: galaxies: dwarf – galaxies: evolution – galaxies: formation – galaxies: individual: UGCA 92 – galaxies: stellar content.

1 INTRODUCTION

Dwarf galaxies are the most numerous objects in the Universe. Knowledge of the star formation processes taking place within them is extremely important for understanding their origin and evolution. The local Universe ($\leq$10 Mpc) is particularly important and convenient for studying dwarf galaxies. Nearby galaxies can be resolved into individual stars, which allows us to study the stellar populations of these galaxies directly. In recent decades, significant progress has been made in the study of resolved stellar populations through use of the *Hubble Space Telescope* (*HST*) and new large ground-based telescopes.

About 50 per cent of nearby galaxies are situated in groups and clouds (Makarov & Karachentsev 2011). Taking into account loose associations of dwarf galaxies (Tully et al. 2006), most of the galaxies within 3 Mpc are not isolated objects. The nearby group around IC 342 is obscured by strong Galactic extinction (see Fig. 1). The IC 342–Maffei complex should have a significant impact on the dynamics and evolution of the nearby Universe. Unfortunately, the 'Zone of Avoidance' hides this region from us, and determination of the main properties of the galaxies behind it is a challenge.

In the framework of the study of the structure of the nearby Universe (*HST* project 9771), we obtained images of dwarf galaxies within the IC 342–Maffei complex. In the present paper we consider the star formation history of the dwarf irregular galaxy UGCA 92, which has for a long time been considered to be the closest neighbour of the nearest starburst galaxy NGC 1569 (Karachentsev, Tikhonov & Sazonova 1994b; Makarova & Karachentsev 2003).

The small irregular galaxy UGCA 92 was discovered by Nilson (1974) and independently catalogued as a possible planetary nebula by Ellis, Grayson & Bond (1984). CCD observations by Hoessel, Saha & Danielson (1988) partially resolving it into individual stars in the g and r passband images were the first to show that UGCA 92 (EGB 0427+63) is a dwarf irregular galaxy. Hodge & Miller (1995) detected 25 H II regions within UGCA 92, concentrated in two well-separated regions of the galaxy. The reddening, measured from the emission-line spectra for bright H II regions, is $E(B-V) = 0.90 \pm 0.08$, and the mean oxygen abundance is about 13 per cent solar, with an

★E-mail: lidia@sao.ru

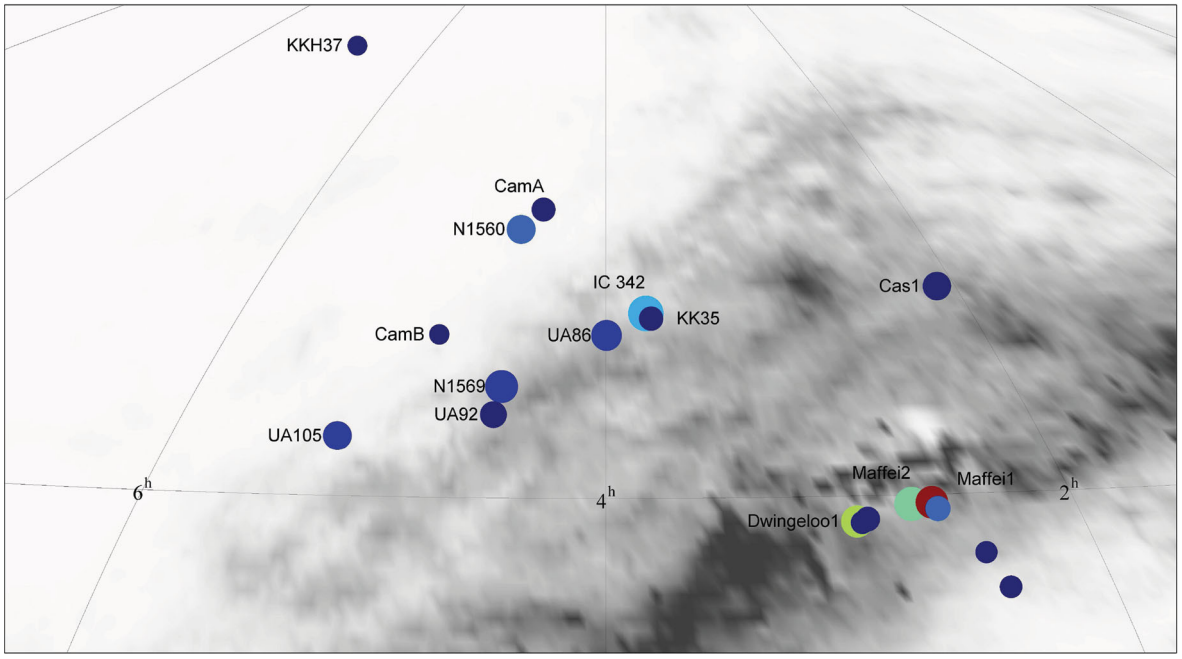

Figure 1. Location of the IC 342–Maffei complex of galaxies in Galactic coordinates. Colours denote galaxy type. The *IRAS* extinction map is shown in grey-scale.

uncertainty of 50 per cent. Karachentsev & Kaisin (2010) carried out Hα flux measurement for UGCA 92 and derived a current star formation rate (SFR) of log (SFR) $= -1.51$ M$_\odot$ yr^{-1}.

The general parameters of UGCA 92 are presented in Table 1. The total magnitudes, colours and central surface brightnesses, $\mu(0)$, are not corrected for Galactic extinction.

2 THE DATA SET

The dwarf irregular galaxy UGCA 92 was observed with the *HST* using the Advanced Camera for Surveys (ACS) on 28 March 2004 (SNAP 9771, PI I. Karachentsev). Two exposures were made with the filters *F*606*W* (1200 s) and *F*814*W* (900 s). An ACS image of the dwarf galaxy is shown in Fig. 2. The photometry of resolved stars in the galaxy was performed with the ACS module of the DOLPHOT package[1] for crowded field photometry (Dolphin 2002) using the recommended recipe and parameters. Only stars with photometry of good quality were included in the final list, following recommendations given in the DOLPHOT User's Guide. We selected stars with signal-to-noise (S/N) ≥ 5 in both filters, $\chi^2 \leq 2.5$ and $|sharp| \leq 0.3$. The resulting colour–magnitude diagram (CMD) contains 32 699 stars (Fig. 3).

Artificial star tests were performed using the same reduction procedures to estimate photometric errors, completeness and blending effects in the most accurate way. A large library of artificial stars was generated spanning the necessary range of stellar magnitudes and colours so that the distribution of the recovered photometry was adequately sampled. The photometric errors and completeness are presented in Fig. 4. The 1σ photometric precision is 0.07 at $F814W = 25$ mag, and 0.19 at $F814W = 27$ mag. Malmquist bias becomes notable for stars with $F814W > 26.8$ mag. In *F*606*W*, the 1σ photometric precision is 0.06 at 26 mag and 0.18 at 28 mag.

[1] http://purcell.as.arizona.edu/dolphot/

Table 1. General parameters of UGCA 92.

RA(J2000)	$04^h32^m03.5^s$	[2]
Dec. (J2000)	$+63°36'58''$	[2]
Size, arcmin	2.0×1.0	[3]
Linear diameter, kpc	3.1	[1]
$(m-M)_0$, mag	27.41 ± 0.25	[1]
Distance, Mpc	3.03 ± 0.35	[1]
B_T, mag	15.22	[4]
$(B-V)_T$, mag	1.34	[4]
$V_{3'}$, mag	14.55	[5]
$I_{3'}$, mag	12.87	[5]
J_T, mag	12.38	[6]
Ks_T, mag	11.12	[6]
$\mu(0)_B$, mag arcsec^{-2}	25.1	[4]
$\mu(0)_V$, mag arcsec^{-2}	24.18 ± 0.01	[5]
$\mu(0)_I$, mag arcsec^{-2}	22.61 ± 0.01	[5]
$E(B-V)$, mag	0.79 ± 0.13	[7]
A_I, mag	1.54 ± 0.25	[7]
V_{LG}, km s^{-1}	93	[8]
M_B, mag	-15.61	[1]
M_{HI}, M$_\odot$	1.56×10^8	[8]
M_{HI}/L_B	0.55	[8]
Fraction of old stars (12–14 Gyr), per cent	84 ± 7	[1]
Metallicity of old stars, [Fe/H], dex	$-2.0 - -1.5$	[1]
Fraction of young stars (500 Myr), per cent	7.6 ± 0.7	[1]
$\langle$SFR$\rangle$, 12–14 Gyr ago, M$_\odot$ yr^{-1}	$1.2 \pm 0.1 \times 10^{-1}$	[1]
$\langle$SFR$\rangle$, last 500 Myr, M$_\odot$ yr^{-1}	$4.3 \pm 0.6 \times 10^{-2}$	[1]

[1] this work; [2] LEDA; [3] Karachentsev et al. (2004); [4] Karachentseva et al. (1996); [5] Sharina et al. (2008); [6] Vaduvescu et al. (2005); [7] Schlegel et al. (1998); [8] Begum et al. (2008).

3 COLOUR–MAGNITUDE DIAGRAM

All resolved stars are significantly shifted to redder colours owing to the high extinction in the Zone of Avoidance of the Milky Way (MW). The diagram is typical for dwarf irregular galaxies. A

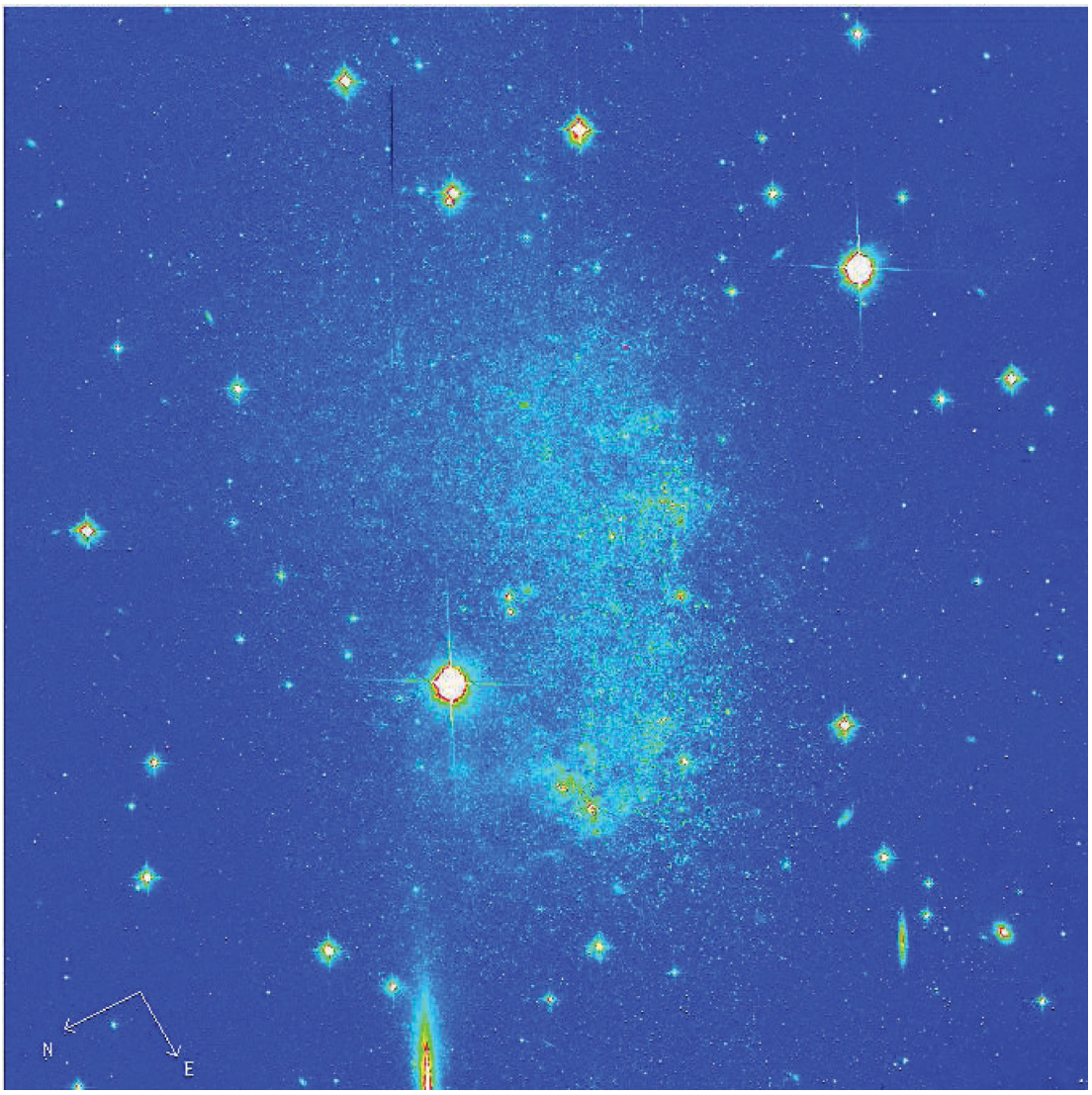

Figure 2. *HST*/ACS image of UGCA 92 in the *F*606*W* filter. The image size is 3.4 × 3.4 arcmin^2.

pronounced upper main sequence (MS) and probable helium-burning blue-loop stars are found at $F606W - F814W < 1.2$ mag. The red supergiant branch (RSG) and the intermediate-age asymptotic giant branch (AGB) are also well populated. The most abundant feature in the CMD is the red giant branch (RGB) (see Fig. 3).

3.1 Extinction

The dwarf galaxy UGCA 92 is situated at Galactic latitude $l = +10\overset{\circ}{.}5$. Galactic extinction in the field of UGCA 92 needs to be addressed in more detail because reddening estimation at low Galactic latitudes in the Zone of Avoidance is highly uncertain (see Schlegel, Finkbeiner & Davis 1998, appendix C). Schlegel et al. (1998) give a colour excess of $E(B - V) = 0.79 \pm 0.13$ using *IRAS*/DIRBE maps of infrared dust emission. We apply this value to the CMD and estimate a mean colour of the upper MS as a first test of the feasibility of the colour excess value. The unreddened $V - I$ colour of upper MS stars is about zero (see Kenyon & Hartmann 1995, for example). We selected MS stars in the appropriate magnitude and colour ranges, namely $|(V - I)_0| \leq 0.5$ and $19.5 \leq I_0 \leq 24.0$. According to our measurements, the mean MS colour is $(V - I)_0 = 0.04$ mag. The colour spread of the MS $\Delta(V - I)_0 = 0.20$ mag is rather large. This spread, as well as the slightly reddish mean MS colour, could indicate the presence of a blue-loop population. The extinction value given by Schlegel et al. (1998) thus seems reasonable, and we do not expect a significant value of internal extinction for this faint dwarf galaxy.

The reddening in UGCA 92 was also determined by Hodge & Miller (1995) from the spectroscopy of 25 bright H II regions within the galaxy. Their reddening value $E(B - V) = 0.90 \pm 0.08$ is in agreement with the value of Schlegel et al. (1998) within uncertainties. The resolution in the *IRAS*/DIRBE maps is 6.1 arcmin (Schlegel et al. 1998). It is considerably larger than the ACS field of view. Therefore, we cannot obtain information about possible variations in extinction across the field of view from these maps. However, a simple test was made using the CMD of UGCA 92. The value of the tip of the RGB (TRGB) was measured in four subframes along the *y*-axis of the whole ACS frame. We found that the TRGB value has

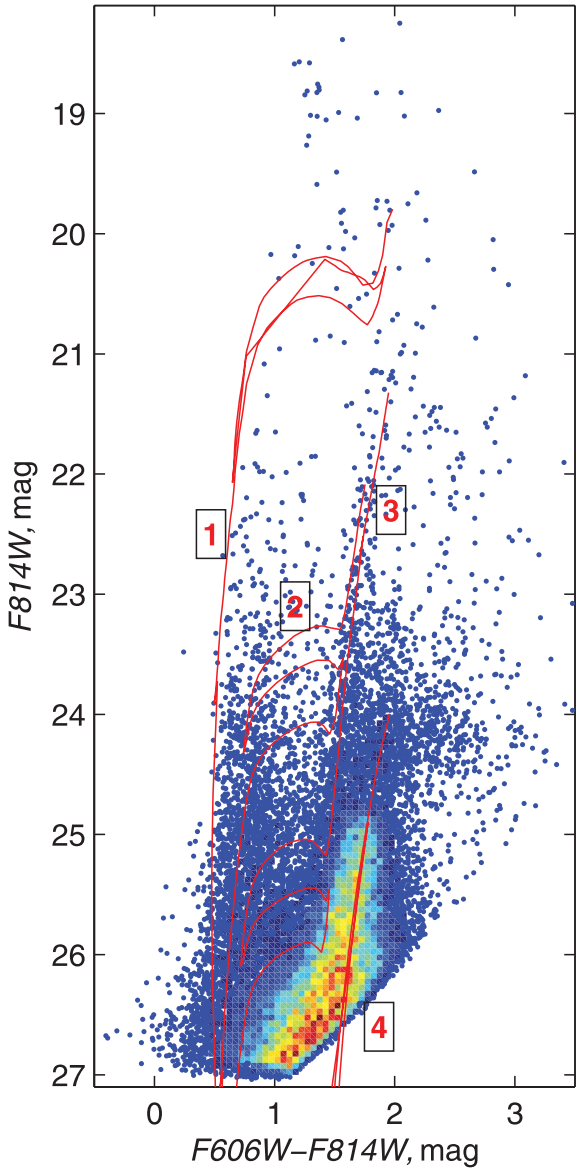

Figure 3. The ($F606W - F814W$), $F814W$ colour–magnitude diagram of the dwarf galaxy UGCA 92. In the dense parts of the diagram the colour represents the density in the Hess diagram, while individual stars are represented where they can be individually distinguished. The magnitudes are not corrected for Galactic extinction. Padova isochrones (Girardi et al. 2000) corresponding to the mean age and metallicity of detected star formation episodes are shown: '1', $Z = 0.008, t = 10$ Myr; '2', $Z = 0.001, t = 50$ Myr; '3', $Z = 0.0004, t = 150$ Myr; '4', $Z = 0.0004, t = 13$ Gyr.

no variations within 1.5σ of the TRGB uncertainty. Consequently, we suggest that there are no variations of external extinction within the ACS field of UGCA 92.

Therefore, we use the colour excess $E(B - V) = 0.79 \pm 0.13$ from Schlegel et al. (1998) in all our measurements in the present paper.

3.2 Foreground contamination

The CMD is highly contaminated by MW stars. To account for this contamination we need to construct the CMD of the MW in the direction of UGCA 92. This information can be obtained from images of neighbouring 'empty' fields. Three fields near to UGCA 92 were found in the *HST* data archive exposed with WFPC2 in the parallel mode (coordinates of the centre are $4^h29^m53^s, +64°42'34''$). However, the photometric limit of these images is about 3 mag higher than the photometric limit of the working UGCA 92 images. To account for the MW contamination in the region of faint stars, we used the TRILEGAL program (Girardi et al. 2005), which computes synthetic CMDs for specified coordinates in the sky and given parameters of MW models. Thus, we use neighbouring field stars to account for the MW contribution to the UGCA 92 CMD brighter than $F814W = 24$ mag and the TRILEGAL synthetic data for the fainter part of the CMD. 30 synthetic CMDs were constructed with TRILEGAL and then averaged to avoid stochastic errors in synthetic CMDs. Random and systematic photometric uncertainties and completeness measured from artificial star experiments were applied to the synthetic CMDs. The resulting contamination by MW stars was determined to be 202 stars over the CMD of UGCA 92.

4 DISTANCE DETERMINATION

The distance of UGCA 92 was first estimated by Karachentsev, Tikhonov & Sazonova (1994a) using the brightest blue and red supergiants as distance indicators. The estimated distance modulus $(m - M)_0 = 26.72$ mag suffered from large photometric uncertainties associated with crowded stellar fields and uncertain reddening. Later, Karachentsev et al. (1997) estimated a distance to UGCA 92 using the same distance indicators and higher-quality data. The resulting distance modulus was $(m - M)_0 = 26.25$ mag. Recently, a more precise distance determination was made using *HST*/ACS data (Karachentsev et al. 2006). A deep CMD permitted the use of the TRGB distance indicator, resulting in a distance modulus of $(m - M)_0 = 27.39$ mag.

However, the TRGB method has recently been considerably improved. We determined the photometric TRGB distance with our TRGBTOOL program, which uses a maximum-likelihood algorithm to determine the magnitude of the tip of the RGB from the stellar luminosity function (Makarov et al. 2006). The estimated value of TRGB is equal to $F814W = 24.84 \pm 0.02$ mag in the ACS instrumental system. The calibration of the TRGB distance indicator has also recently been improved (Rizzi et al. 2007), with the colour dependence of the absolute magnitude of the TRGB and zero-point issues in *HST*/ACS and WFPC2 being addressed. Using this calibration, we obtained the true distance modulus to UGCA 92 of $(m - M)_0 = 27.41 \pm 0.25$ mag and a distance of $D = 3.03 \pm 0.35$ Mpc. Bear in mind that, given the small error of the TRGB measurement (0.02 mag) and the high precision of the calibration (0.02 mag), the resulting accuracy is entirely determined by the uncertainty in foreground extinction of 0.25 mag in the direction of UGCA 92. The CMD with the fitted RGB luminosity function and the resulting TRGB value is shown in Fig. 5.

5 STAR FORMATION HISTORY

The star formation and metal-enrichment history of UGCA 92 has been determined from its CMD using our STARPROBE package. This program adjusts the observed photometric distribution of stars in the CMD against a positive linear combination of synthetic diagrams of single stellar populations (SSPs, single age and single metallicity). Our approach is described in more detail in Makarov & Makarova (2004) and Makarova et al. (2010).

The observed data were binned into Hess diagrams, giving the number of stars in cells of the CMD (two-dimensional histogram).

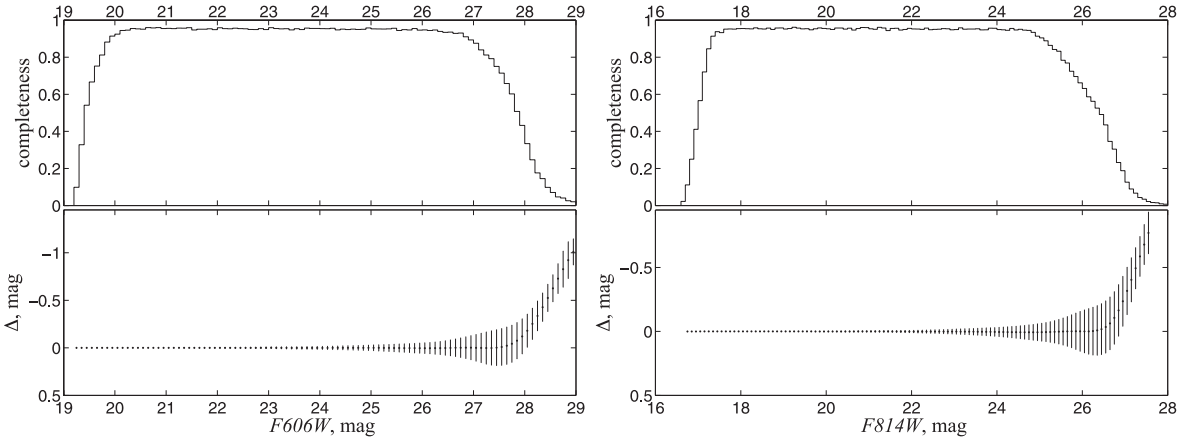

Figure 4. Photometric errors and completeness for UGCA 92. The top panels show the completeness, that is, the fraction of artificial stars recovered within the photometric reduction procedure, as a function of the *F*606*W* and *F*814*W* magnitudes. The bottom panels give the difference between the measured and the true input magnitude (Δmag = measure – input). The error bars are 1σ residuals.

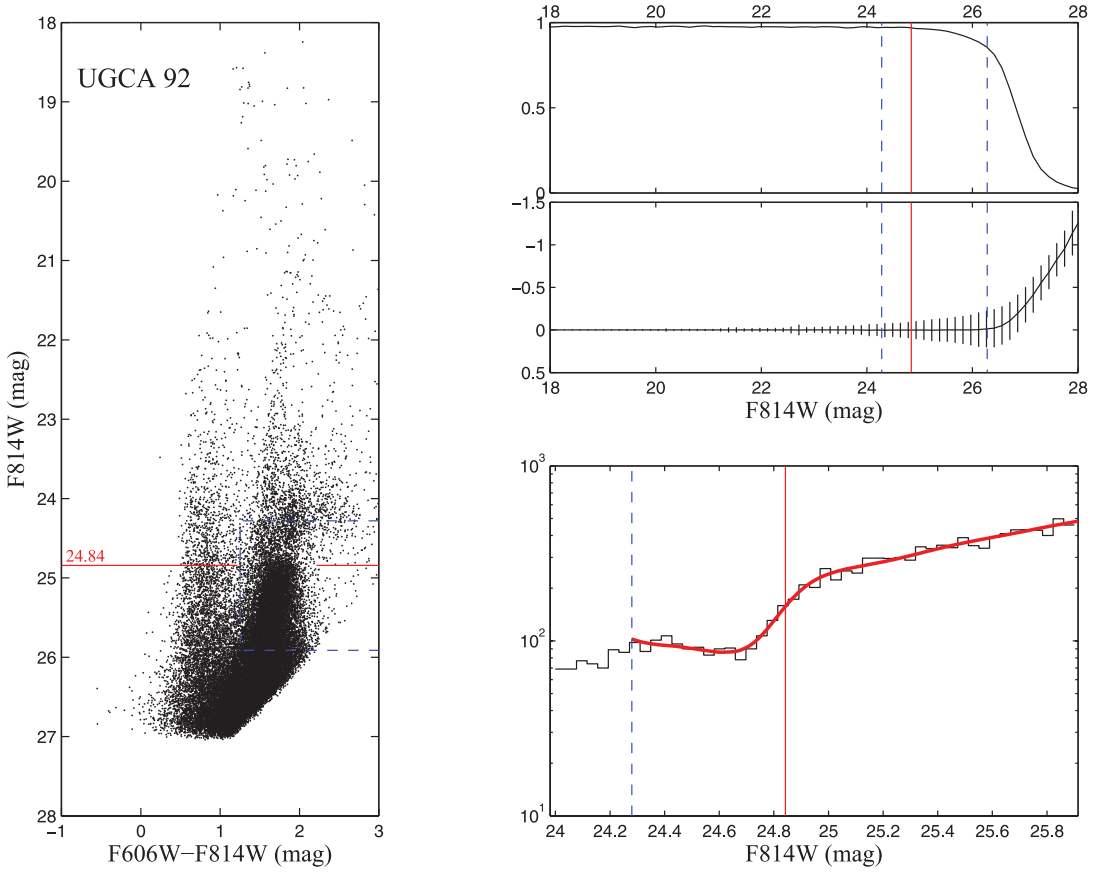

Figure 5. The colour–magnitude diagram (left panel) and the TRGB calculation results for UGCA 92. The upper right panel shows the completeness, photometric errors and dispersion in errors (vertical bars) versus the *HST*/ACS *F*814*W* filter magnitude. The lower right panel gives a histogram of the *F*814*W* luminosity function. The resulting model LF convolved with photometric errors and incompleteness is displayed as a bold solid line with a jump at the position of the TRGB.

The size of the cell is 0.05 mag in each passband. The synthetic Hess diagrams were constructed from theoretical stellar isochrones and initial mass function (IMF). Each artificial diagram is a map of probabilities to find a star in a cell for a given age and metallicity. We used the Padova2000 set of theoretical isochrones (Girardi et al. 2000), and a Salpeter (1955) IMF. The distance was adopted from the present paper (see above), and the Galactic extinction from Schlegel et al. (1998). The synthetic diagrams were altered by the same incompleteness and crowding effects, and photometric systematics, as those determined for the observations using artificial star experiments. We also took into account the presence of unresolved binary stars (binary fraction). Following Barmina, Girardi &

Chiosi (2002), the binary fraction was taken to be 30 per cent. The mass distribution for the secondary was taken to be flat in the range 0.7 to 1.0 of the primary mass. The best-fitting combination of synthetic CMDs is a maximum-likelihood solution taking into account the Poisson noise of star counts in the cells of the Hess diagram. The resulting star formation history is shown in Fig. 6. The 1σ error of each SSP is derived from an analysis of the likelihood function.

According to our measurements, the main star formation event occurred 12–14 Gyr ago with a high mean SFR of $1.2 \pm 0.1 \times 10^{-1}$ $M_\odot$ yr^{-1}. This is the total SFR over the whole galaxy. The metallicity range for most stars formed during this event is [Fe/H] = [−2.0 : −1.5] dex. This initial burst accounts for about 84±7 per cent of the total mass of formed stars.

The quiescent period occurred about 6 to 12 Gyr ago. However, the absence of star formation activity in this period could be a result of the tight packing of the different-age stars in the upper part of the RGB. At a distance of 3 Mpc, fainter stellar populations, such as the horizontal branch and lower part of the MS, are hardly resolved with the *HST*. Without these details it is difficult to resolve an age–metallicity–SFR relation for the oldest (>6–8 Gyr) star formation events, because of the tight packing of the corresponding isochrones for the brightest part of the CMD.

There are signs of marginal (insignificant) star formation 4–6 Gyr ago. The metallicity of these stars is similar to the metal abundance of the oldest stellar population.

There are also indications of recent star formation starting about 1.5–2 Gyr ago and continuing to the present. We measured the star formation history in short age periods throughout the last 500 Myr to provide more detail for the recent and ongoing star formation. The mean SFR of the stars formed in the last 50 Myr is $3.9 \pm 0.6 \times 10^{-2}$ $M_\odot$ yr^{-1}. This ongoing SFR is in good agreement with the independent estimation by Karachentsev & Kaisin (2010) from Hα flux measurements ($3.2 \pm 0.3 \times 10^{-2}$ $M_\odot$ yr^{-1}). The recent star formation shows moderate enhancement from ∼ 200 to 300 Myr. The mean SFR in the last 500 Myr is $4.3 \pm 0.6 \times 10^{-2}$ $M_\odot$ yr^{-1}. The mass portion of stars formed in the last 500 Myr is 7.6 ± 0.7 per cent of the total stellar mass. The metallicity of the recent star formation event is determined with large uncertainty owing to the relatively poor statistics in comparison with the more numerous old stars. However, the measurements show that a significant fraction of the young stars are evidently metal-enriched. It is very likely that the ongoing star formation has an associated metallicity of −0.6 to −0.3 dex.

5.1 Spatial distribution of stellar populations

We selected a few stellar populations depending on their position in the CMD. The results of this selection are presented in Fig. 7. The upper MS stars (upper left panel) have an unreddened colour $(V - I)_0 \leq 0$, and their age range is about 10–100 Myr. These youngest stars of the galaxy are concentrated mainly in a few knots, which highlight regions of ongoing star formation and form the irregular structure of UGCA 92.

In the upper right panel of the figure we show supposed blue-loop stars selected by a colour $0.0 \leq (V - I)_0 \leq 0.5$. Their age range is ∼10–200 Myr. The spatial distribution of these stars is considerably smoother and more regular in comparison with MS stars, although they are concentrated in the central parts of the galaxy.

The selection criterion for red supergiant stars, with ages in the range ∼10 Myr to 1 Gyr (lower left panel), was quite conservative,

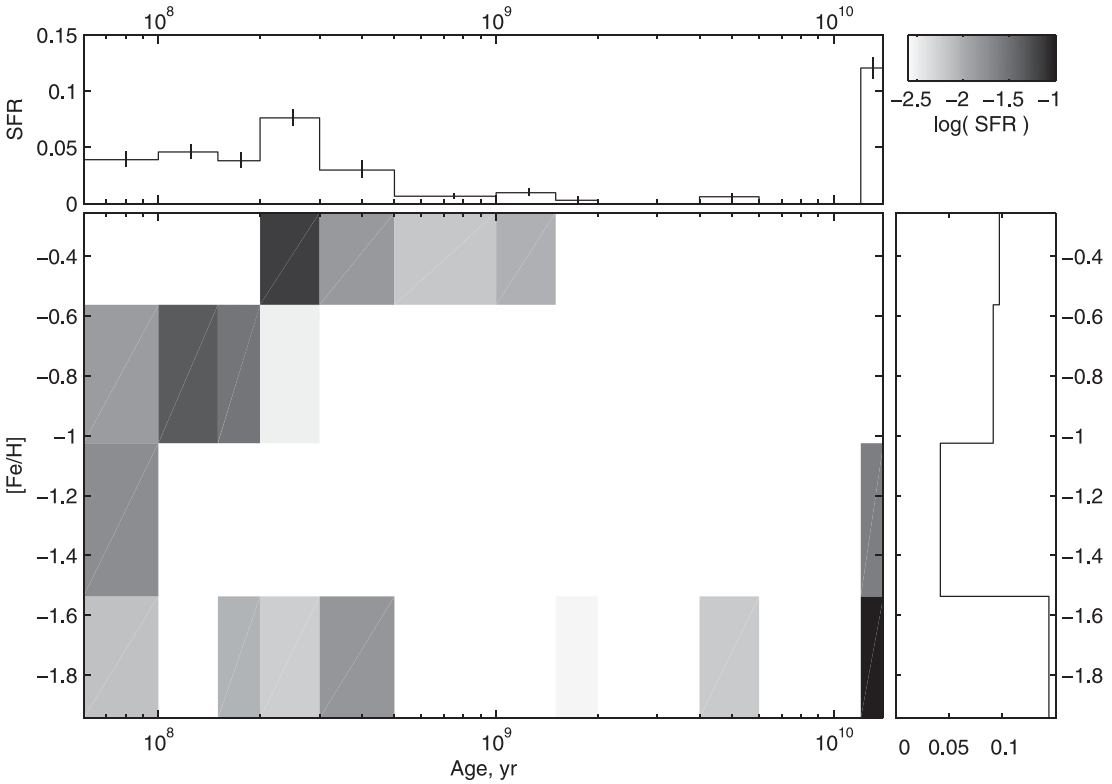

Figure 6. The star formation history of the dwarf irregular galaxy UGCA 92. The top panel shows the star formation rate (SFR) ($M_\odot$ yr^{-1}) against the age of the stellar populations. The bottom panel represents the metallicity of stellar content as a function of age. The colour corresponds to the strength of the SFR for a given age and metallicity.

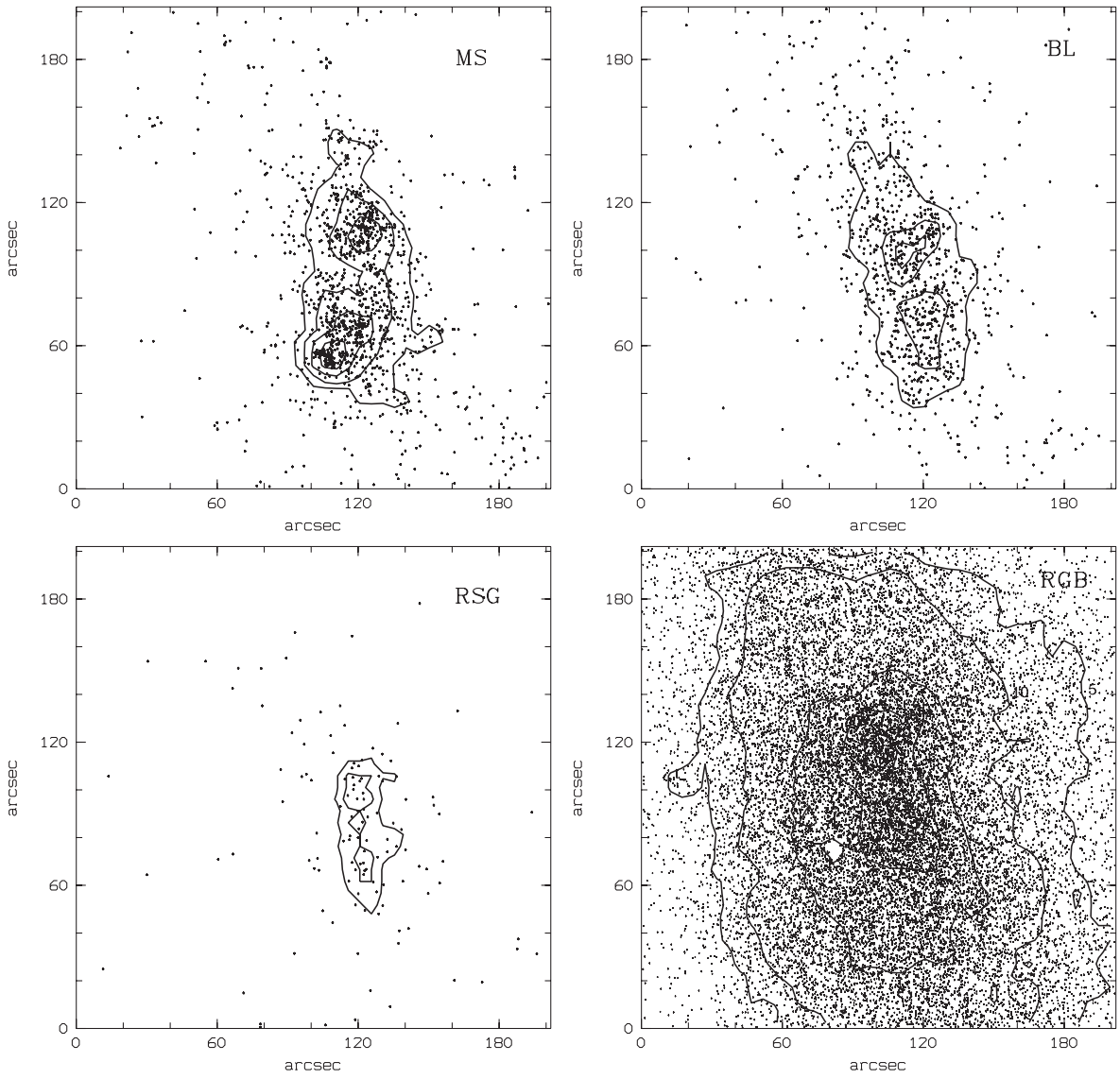

Figure 7. Spatial distribution of the stellar populations in UGCA 92. The main sequence stars are bounded by $(V-I)_0 \leq 0$. The boundaries of the shown blue-loop are $0.0 \leq (V-I)_0 \leq 0.5$. RS stars correspond to the range $1.0 \geq (V-I)_0 \leq 1.5$ and $I_0 \leq 21.5$. The red giant population is bounded by $(V-I)_0 \geq 0.5$ and $I_0 \geq 23.0$. Stellar density contours of the populations are shown with solid lines.

namely $1.0 \leq (V-I)_0 \leq 1.5$ and $I_0 \leq 21.5$, to avoid possible contamination of the spatial structure by young and intermediate-age AGB stars (which are redder) and RGB stars (which are fainter). As a result, the selected population is not numerous, and is smoothly distributed in the central part of the galaxy, nearly along the major axis.

The most numerous population is the RGB (>1 Gyr) observed at approximately $(V-I)_0 \geq 0.5$ and $I_0 \geq 23.0$. The stars are widely distributed in the image, with apparent concentration in the centre of UGCA 92 and close to the major axis. The density of the stars is smoothly decaying to the edge of the galaxy, which probably extends beyond the image boundary.

6 STAR FORMATION AND ENVIRONMENT

IC 342–Maffei is a highly obscured nearby galaxy complex. These galaxies are split into two groups. One group surrounds the giant face-on galaxy IC 342 and the other surrounds the pair of E+S galaxies Maffei 1 and Maffei 2. According to Karachentsev (2005), the groups contain eight members each. It should be noted that the distances to the group members could be highly uncertain owing to the high uncertainty of the Galactic extinction in this direction. The IC 342 group structure is shown in Fig. 8. There are 19 galaxies in the plot situated at distances ≤1.8 Mpc from IC 342. The distances were taken from the Catalog of Neighboring Galaxies (Karachentsev et al. 2004). The data on the distances were updated recently (Karachentsev, private communication). The two galaxy groups, surrounding IC 342 and surrounding Maffei 1 and Maffei 2, can be seen in the figure. Most of the complex members are dwarf galaxies. The morphological types of the objects are coded by colour according to de Vaucouleurs et al. (1991) and Karachentsev et al. (2004), from early types (red) to late types (dark blue). It is interesting to note that all the dwarf satellites of IC 342, including the galaxy under study, UGCA 92, are irregulars. The absence of a dwarf spheroidal satellite subsystem in the group could imply that dSphs were not discovered, because their lower surface brightness

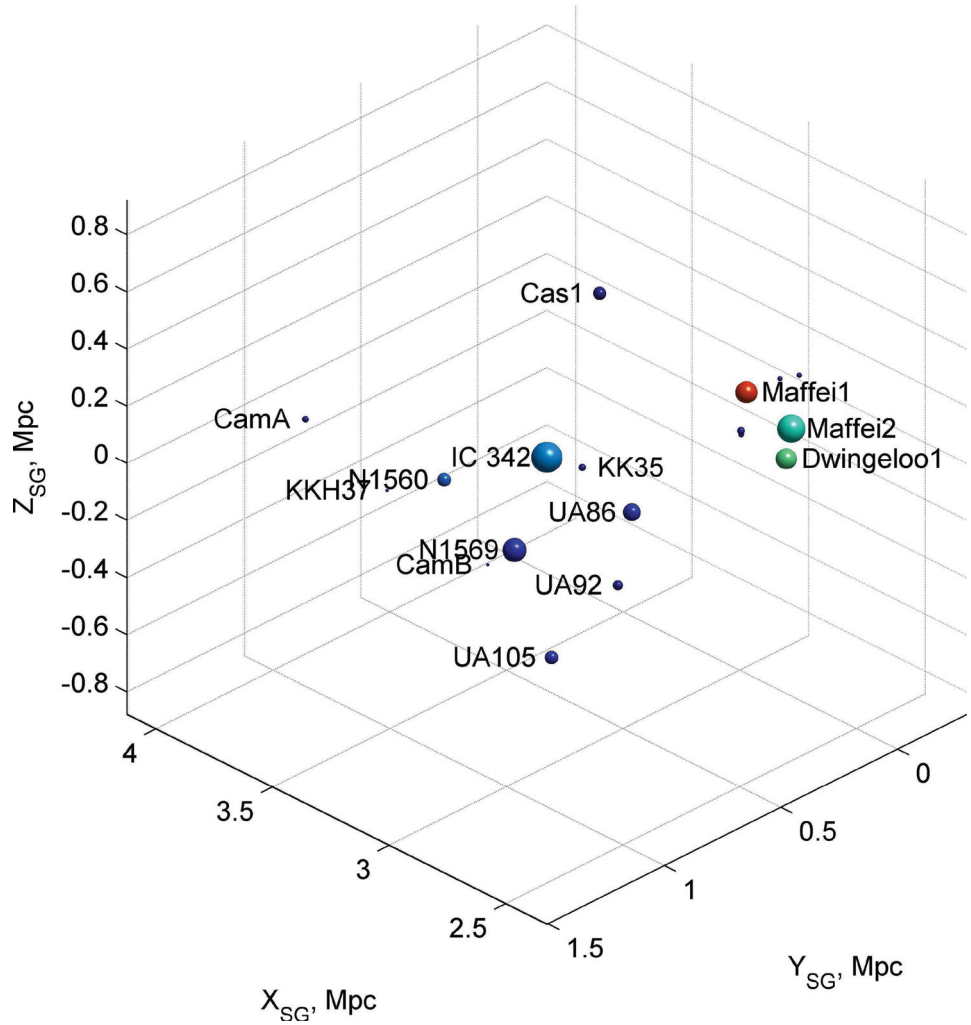

Figure 8. The 3D structure of the IC 342 group. The size of the data cube is 1.8 × 1.8 × 1.8 Mpc^3. The giant spiral IC 342 is placed in the centre of the cube.

and high Galactic extinction placed serious constraints on observations.

The dwarf irregular galaxy under study, UGCA 92, is situated at a linear distance $D = 440$ kpc from the gravitational centre of the group IC 342. The three galaxies nearest to UGCA 92 are UGCA 86 (linear distance $D = 260$ kpc), UGCA 105 ($D = 300$ kpc) and NGC 1569 ($D = 360$ kpc). UGCA 92 is often considered to be the companion to the starburst galaxy NGC 1569. They are known to have similar radial velocities, $V_{LG} = 93$ km s^{-1} for UGCA 92 (Begum et al. 2008) and $V_{LG} = 106$ km s^{-1} for NGC 1569 (Walter et al. 2008). Indeed, except for the giant spiral IC 342 ($D = 320$ kpc from NGC 1569) and a very small irregular galaxy Cam B ($D = 190$ kpc from NGC 1569), UGCA 92 is the spatially closest companion to NGC 1569. The median radial velocity of galaxies within the IC 342 group is $V_{LG} = 244$ km s^{-1}, with a velocity dispersion of 79 km s^{-1}. The pair of galaxies NGC 1569–UGCA 92 has the maximal peculiar velocity within the group. The question arises whether these galaxies form a real subsystem within the IC 342 group. Indeed, the uncertainty in the UGCA 92 distance is 350 kpc (see Table 1), which is close to the derived linear separation between NGC 1569 and UGCA 92. The main source of this uncertainty is the huge Galactic absorption. Taking into account the close radial velocities and close positions on the sky, these galaxies could form a tight physical pair. In this case we could expect to find a correlation in their star formation. On the other hand, the estimation of the linear distance between the galaxies is reasonable. Therefore, the similar velocities and positions on the sky could just be coincidences in a virialized system.

NGC 1569 is the well-known nearest strong starburst galaxy. Vallenari & Bomans (1996) found evidence of a recent burst of star formation from about 15 to 4 Myr ago. Another distinct burst not longer than 150 Myr ago was also found. Later, Angeretti et al. (2005) found three recent distinct starbursts using *HST*/NICMOS data: 13–37 Myr, 40–150 Myr and ∼1 Gyr ago (for 2.2 Mpc distance). The presence of bright H II regions also indicates substantial ongoing star formation. The galaxy contains two extremely luminous super-star clusters (Hunter et al. 2000). In this latter work, 45 other young clusters were also identified, most of them having an age <30 Myr. The distance to this galaxy was uncertain for a long time. An accurate TRGB distance (3.36 ± 0.20 Mpc) was measured by Grocholski et al. (2008) using *HST*/ACS images. Furthermore, the stellar content of the NGC 1569 halo was studied in great detail recently by Ryś et al. (2011). Judging from these two papers, the old (about 10 Gyr) RGB stars, including the outer halo in this starburst galaxy, should be more metal-rich ([Fe/H] $\simeq -1$) than we measured for the old RGB stars of UGCA 92. One of the interesting conclusions of Ryś et al. (2011) is that the outer stellar halo of the starburst galaxy NGC 1569 is not tidally truncated and is not an outward

extension of the inner disc. Rather, it is a distinct stellar halo with no evident age/metallicity gradient; that is, the starburst phenomenon is highly centrally concentrated. Such a morphology could be the result of past interaction/merging. The question arises whether we can find any signs of past interactions for the dwarf galaxies using the information on the star formation of these objects.

In addition to UGCA 92, in the subgroup of the closest neighbours NGC 1569–UGCA 92–UGCA 86–UGCA 105, only UGCA 86 has observations deep enough (*HST*/ACS images within project number 9771, PI I. Karachentsev) to judge overall star formation from the photometry of resolved stars. The CMD of this galaxy is presented in Fig. 9. UGCA 92 ($D = 3.03$ Mpc) and UGCA 86 ($D = 2.96$ Mpc, Karachentsev et al. 2006) are at nearly the same distance from us. However, UGCA 86 has the brighter absolute stellar magnitude ($M_B = -17.95$) and larger angular size. We measured more resolved stars in the ACS field. An upper MS and helium-burning blue-loop stars are found at $F606W - F814W < 1.6$ mag. The well-populated RSG and the huge AGB are situated above the TRGB at $F606W - F814W > 1.6$ mag and $F814W < 25.14$ mag. Galactic extinction for UGCA 86 is even higher [$E(B - V) = 0.94$ mag according to Schlegel et al. (1998)]. The photometric limit and large colour excess seriously affect the RGB zone in the CMD (see Fig. 9). This fact significantly reduces the reliability of a computational modelling of star formation older than 1 Gyr. Therefore, we only made a fitting of theoretical isochrones to the young stellar population of UGCA 86. The age and metallicity of these populations are similar in UGCA 86 and UGCA 92.

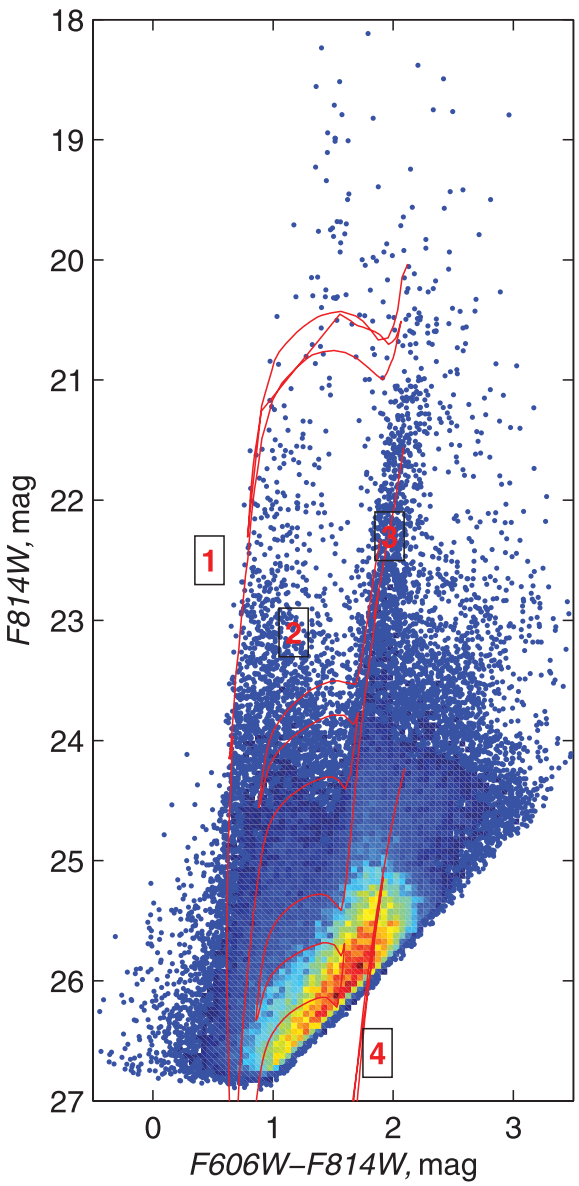

Figure 9. The ($F606W - F814W$), $F814W$ CMD of the dwarf galaxy UGCA 86. The magnitudes are not corrected for Galactic extinction. The same Padova theoretical isochrones (Girardi et al. 2000) as for the UGCA 92 CMD are shown.

H I and Hα observations of NGC 1569, UGCA 92 and UGCA 86 have been performed by various authors. Numerous Hα knots have been detected in all three galaxies, tracking the ongoing star formation events in these objects (Hodge & Miller 1995; Kingsburgh & McCall 1998; Karachentsev & Kaisin 2010). High-sensitivity H I maps of NGC 1569 show evidence for a companion H I cloud connected to the galaxy by a low surface brightness H I bridge. At the edge of NGC 1569 it coincides with H I arcs (Stil & Israel 1998). The hydrogen cloud is apparently not correlated with any optical satellites/counterparts. Stil & Israel (2002) argued that about 10 per cent by mass of all H I in NGC 1569 has unusually high velocities. Some of this H I may be associated with the mass outflow evident from Hα measurements, but some may also be associated with the NGC 1569 H I companion and H I bridge, in which case infall rather than outflow might be the cause of the discrepant velocities. H I observations by Stil, Gray & Harnett (2005) show a complex structure for UGCA 86, with two separate components: a rotating disc and a highly elongated spur that is kinematically disjunct from the disc.

Summarizing the cited results, we could conclude that hydrogen at the outskirts of the starburst galaxy NGC 1569 is highly disturbed with signs of infall, but no similar features were detected in the neighbouring dwarfs UGCA 92 and UGCA 86.

It should be noted that all the data known to date cannot give us the particular time at which the series of distinct intensive starbursts in NGC 1569 started. Angeretti et al. (2005) note that the last starburst should have occurred 8–27 Myr ago if the distance to the galaxy were 2.9 Mpc, instead 13–37 Myr when assuming a distance of 2.2 Mpc. The revised accurate distance to NGC 1569 according to Grocholski et al. (2008) is 3.36 Mpc. It is possible that the two other starburst periods occurring 40–150 Myr ago and about 1 Gyr ago will be shifted to younger ages assuming the new distance. Our data on recent star formation in the companion UGCA 92 galaxy show substantial and continuous star formation in the last 500 Myr, with enhancement at about 200–300 Myr. Therefore, our results do not indicate a direct connection between the recent star formation in the two galaxies.

7 CONCLUSIONS

We have derived a quantitative star formation history of the dwarf irregular galaxy UGCA 92 situated in the highly obscured nearby galaxy group IC 342. Owing to the low Galactic latitude ($l = +10.^{\circ}5$), the extinction is very high [$E(B - V) = 0.79 \pm 0.13$ according to Schlegel et al. (1998)] in this direction. The star formation history was reconstructed using *HST*/ACS images of the galaxy and resolved stellar population modelling. According to our measurements, 84 per cent of the total stellar mass was formed during the star formation occurring about 12–14 Gyr ago. The metallicity range of these stars is [Fe/H] = [−2.0 : −1.5] dex. There are also signs of marginal star formation 4–6 Gyr ago. The metallicity of

these stars is similar to the metal abundance of the oldest stellar population.

UGCA 92 has a typical morphology of an irregular dwarf with apparent associations of bright blue stars in its body. Numerous H II knots were also detected in the galaxy, tracking the ongoing star formation. According to our measurements, recent star formation started about 1.5–2 Gyr ago and continues to the present. We modelled the star formation history with good time resolution for the recent star formation event. The continuous star formation in this period shows moderate enhancement from about 200 to 300 Myr ago. The mean SFR in the last 500 Myr is $4.3 \pm 0.6 \times 10^{-2}$ $M_\odot$ yr^{-1}, and in the last 50 Myr is $3.9 \pm 0.6 \times 10^{-2}$ $M_\odot$ yr^{-1}. The mass portion of stars formed in the last 500 Myr is 7.6 per cent of the total mass of formed stars. The metallicity of the recent star formation event is determined with a large uncertainty owing to the relatively poor statistics in comparison with the more numerous old stars. However, the measurements show that a significant fraction of the young stars are metal-enriched. It is very likely that the ongoing star formation has a metallicity of -0.6 to -0.3 dex.

UGCA 92 is often considered to be the companion to the starburst galaxy NGC 1569. They are known to have similar radial velocities, $V_{LG} = 93$ km s^{-1} for UGCA 92 (Begum et al. 2008) and $V_{LG} = 106$ km s^{-1} for NGC 1569 (Walter et al. 2008). The linear distance between the galaxies is $D = 360$ kpc. These two objects evidently could be considered as a close pair of galaxies.

Another dwarf galaxy close to UGCA 92 is UGCA 86, with a linear distance of $D = 260$ kpc. Our *HST*/ACS data allow us to analyse overall star formation from the photometry of resolved stars. Theoretical isochrone fitting shows an apparent similarity of the resolved stellar populations in the two galaxies.

It is worthwhile to note that the mean metallicity of the old RGB stars measured by us in UGCA 92 is lower than the known metallicity of the halo RGB stars in NGC 1569.

A comparison of our star formation history of UGCA 92 with that of NGC 1569 reveals no causal or temporal connection between recent star formation events in these two galaxies. We suggest that the starburst phenomenon in NGC 1569 is not related to the closest dwarf neighbours and does not affect their star formation history.

Probably, detailed N-body modelling of the group within 300 kpc of IC 342 will be necessary to clarify the reason for recent starbursts in NGC 1569.

ACKNOWLEDGMENTS

This work is based on observations made with the NASA/ESA *Hubble Space Telescope* and obtained from the data archive at the Space Telescope Science Institute. STScI is operated by the Association of Universities for Research in Astronomy, Inc. under NASA contract NAS 5-26555. The work was supported by the Russian Foundation for Basic Research (RFBR) grant 11–02–00639 and Russian–Ukrainian RFBR grant 11–02–90449. We acknowledge the support of the Ministry of Education and Science of the Russian Federation under contract 14.740.11.0901. This work was partially supported by the Physical Sciences Department programme of the Russian Academy of Sciences. We are grateful to the anonymous referee for very useful comments on the paper, and to Scott Trager for his kind help with text preparation. We acknowledge use of the HyperLEDA data base (http://leda.univ-lyon1.fr) (Paturel et al. 2003).

REFERENCES

Angeretti L., Tosi M., Greggio L., Sabbi E., Aloisi A., Leitherer C., 2005, AJ, 129, 2203
Barmina R., Girardi L., Chiosi C., 2002, A&A, 385, 847
Begum A., Chengalur J. N., Karachentsev I. D., Sharina M. E., Kaisin S. S., 2008, MNRAS, 386, 1667
Dolphin A. E., 2002, MNRAS, 332, 91
Ellis G. L., Grayson E. T., Bond H. E., 1984, PASP, 96, 283
Girardi L., Bressan A., Bertelli G., Chiosi C., 2000, A&AS, 141, 371
Girardi L., Groenewegen M. A. T., Hatziminaoglou E., da Costa L., 2005, A&A, 436, 895
Grocholski A. J. et al., 2008, ApJ, 686, L79
Hodge P., Miller B. W., 1995, ApJ, 451, 176
Hoessel J. G., Saha A., Danielson G. E., 1988, PASP, 100, 680
Hunter D. A., O'Connell R. W., Gallagher J. S., Smecker-Hane T. A., 2000, AJ, 120, 2383
Karachentsev I., Drozdovsky I., Kajsin S., Takalo L. O., Heinamaki P., Valtonen M., 1997, A&AS, 124, 559
Karachentsev I. D., 2005, AJ, 129, 178
Karachentsev I. D., Kaisin S. S., 2010, AJ, 140, 1241
Karachentsev I. D., Tikhonov N. A., Sazonova L. N., 1994a, Astron. Lett., 20, 84
Karachentsev I. D., Tikhonov N. A., Sazonova L. N., 1994b, A&AS, 106, 555
Karachentseva V. E., Prugniel P., Vennik J., Richter G. M., Thuan T. X., Martin J. M., 1996, A&AS, 117, 343
Karachentsev I. D., Karachentseva V. E., Huchtmeier W. K., Makarov D. I., 2004, AJ, 127, 2031
Karachentsev I. D. et al., 2006, AJ, 131, 1361
Kenyon S. J., Hartmann L., 1995, ApJS, 101, 117
Kingsburgh R. L., McCall M. L., 1998, AJ, 116, 2246
Makarov D., Karachentsev I., 2011, MNRAS, 412, 2498
Makarov D., Makarova L., Rizzi L., Tully R. B., Dolphin A. E., Sakai S., Shaya E. J., 2006, AJ, 132, 2729
Makarov D. I., Makarova L. N., 2004, Astrophysics, 47, 229
Makarova L., Koleva M., Makarov D., Prugniel P., 2010, MNRAS, 406, 1152
Makarova L. N., Karachentsev I. D., 2003, Astrophysics, 46, 144
Nilson P., 1974, Catalogue of Selected Non-Ugc Galaxies, Uppsala Astron. Obs. Rep. 5
Paturel G., Petit C., Prugniel Ph., Theureau G., Rousseau J., Brout M., Dubois P., Cambrésy L., 2003, A&A, 412, 45
Rizzi L., Tully R. B., Makarov D., Makarova L., Dolphin A. E., Sakai S., Shaya E. J., 2007, ApJ, 661, 815
Ryś A., Grocholski A. J., van der Marel R. P., Aloisi A., Annibali F., 2011, A&A, 530, A23
Salpeter E. E., 1955, ApJ, 121, 161
Schlegel D. J., Finkbeiner D. P., Davis M., 1998, ApJ, 500, 525
Sharina M. E. et al., 2008, MNRAS, 384, 1544
Stil J. M., Israel F. P., 1998, A&A, 337, 64
Stil J. M., Israel F. P., 2002, A&A, 392, 473
Stil J. M., Gray A. D., Harnett J. I., 2005, ApJ, 625, 130
Tully R. B. et al., 2006, AJ, 132, 729
Vaduvescu O., McCall M. L., Richer M. G., Fingerhut R. L., 2005, AJ, 130, 1593
Vallenari A., Bomans D. J., 1996, A&A, 313, 713
de Vaucouleurs G., de Vaucouleurs A., Corwin H. G., Jr, Buta R. J., Paturel G., Fouque P., 1991, in de Vaucouleurs G., de Vaucouleurs A., Corwin H. G., Jr, Buta R. J., Paturel G., Fouque P., eds, Third Reference Catalogue of Bright Galaxies. Springer-Verlag, Berlin
Walter F., Brinks E., de Blok W. J. G., Bigiel F., Kennicutt R. C., Jr, Thornley M. D., Leroy A., 2008, AJ, 136, 2563

This paper has been typeset from a TEX/LATEX file prepared by the author.